

## CHAPTER 3

# METHODS

### APPROACH TO THE PROBLEM

Limited evidence is available describing the effect of age on the  $\dot{V}O_2$  and  $mOxy$  responses to various exercise intensities. Even fewer data are available reporting the effect of age on  $\dot{V}O_2$  and  $mOxy$  responses in trained individuals. The present series of studies were designed to identify a possible aging effect on the  $\dot{V}O_2$  and  $mOxy$  kinetic responses in trained cyclists. Previous research investigating the effect of age on these responses have used aged groups unmatched for  $\dot{V}O_{2max}$  and training status, both of which have been shown to influence the metabolic response to exercise.

In the present series of studies, Study One was designed to match the young and middle-aged cyclists on physiological capacities and peripheral muscle characteristics. The three subsequent studies (2-4) were designed to investigate the effects of age on the  $\dot{V}O_2$  and  $mOxy$  on-transient, slow component and off-transient responses, respectively. Further aims of this series of studies were to relate the  $\dot{V}O_2$  and  $mOxy$  responses to changes in a number of hematological parameters measured across a series of SWT of increasing intensity. The current series of studies aimed to relate these responses to the peripheral muscle characteristics described within Study One. Lastly, Study Three aimed to relate the  $\dot{V}O_2$  and  $mOxy$  slow components to changes in muscle activation and fibre recruitment using novel methodological techniques which have previously not been utilised.

## **SUBJECTS**

Young (18-25 y; n=7) and middle-aged (45-55 y; n=7) cyclists were recruited from the local cycling and triathlon community to participate in the current series of studies. Criteria for inclusion were that they had been consistently training for competitive cycling or triathlon over the previous 12 months. All subjects gave verbal and written informed consent after a full explanation of the requirements and risks of all testing procedures (Appendix 1). Prior to participation, all cyclists were screened for cardiovascular risk factors using a revised Physical Activity Readiness Questionnaire (r-PARQ) which was based upon the criteria established by the American College of Sports Medicine (Appendix 2). All experimental procedures and consent mechanisms were granted approval by the Central Queensland University Human Research Ethics Committee (Appendix 3).

### **Anthropometry**

Prior to exercise testing, a restricted anthropometric profile was performed on each cyclist by a trained anthropometrist using the procedures described by Norton and Olds (1996). Stature was measured to the nearest 0.1 cm with a fixed *Blaydon* stadiometer (Lugarna, NSW, Australia) and body mass to the nearest 0.1 kg using previously-calibrated electronic scales (Tanita Corporation, Tokyo, Japan). The sum of nine skinfolds ( $\sum 9$  SF) was measured with *Harpender* skinfold calipers (John Bull Instruments, West Sussex, UK) to the nearest 0.1 mm. The nine skinfold sites included triceps, biceps, subscapular, supraspinale, mid-axilla, iliocristale, abdominal, medial thigh and calf. Girth measurements included arm (relaxed), arm (flexed), hip, waist and maximal calf and were measured to the nearest 0.1 mm with a *Lufkin Executive*

tape (CooperTools, Apex, NC, USA). Humeral and femoral bone breadths were measured to the nearest 0.1 cm using *Rosscraft Campbell* bone calipers (Rosscraft Campbell, Canada). All anthropometric calculations ( $\Sigma 9$  SF, % body fat and lean body mass) were performed using the *Lifesize* software (Human Kinetics, Lower Mitcham, SA, Australia). The intra-tester reliability of the anthropometrist was acceptable for skinfold measurement (TEM: 0.9 mm; TEM%: 0.25%).

## **EXERCISE PROTOCOLS**

Each subject completed six visits to the School of Health and Human Performance Laboratory within a three-week period, and a seventh visit to the local hospital. The six laboratory sessions included familiarisation, assessment of ventilatory threshold (VT) and maximal aerobic power ( $VO_{2max}$ ), three repeat square wave transition (SWT) sessions and a 30 minute time trial (30TT). The testing sequence is presented as Figure 3.1.

All testing sessions were performed at the same time of day in order to avoid any circadian influence. Prior to each testing session, subjects were instructed to eat a carbohydrate-rich meal within 12 h prior to testing; abstain from caffeine and alcohol for 4 h prior to testing and to refrain from physical training for at least 24 h prior to testing. All exercise testing was conducted on an electromagnetically-braked cycle ergometer (Excalibur, Lode, Groningen, The Netherlands) which was interfaced to a programmable workload control box. Each cyclist used their own personal cycling shoes and cleats. Subjects were instructed to maintain a cadence of 90 RPM, as this closely matches the preferred cadence of trained cyclists (Marsh and Martin 1997). The

standardisation of cadence also allowed neuromuscular responses to be comparable across all exercise tests. All laboratory testing conditions were performed in a standardised environment at  $22 \pm 2$  °C and  $< 70\%$  relative humidity.

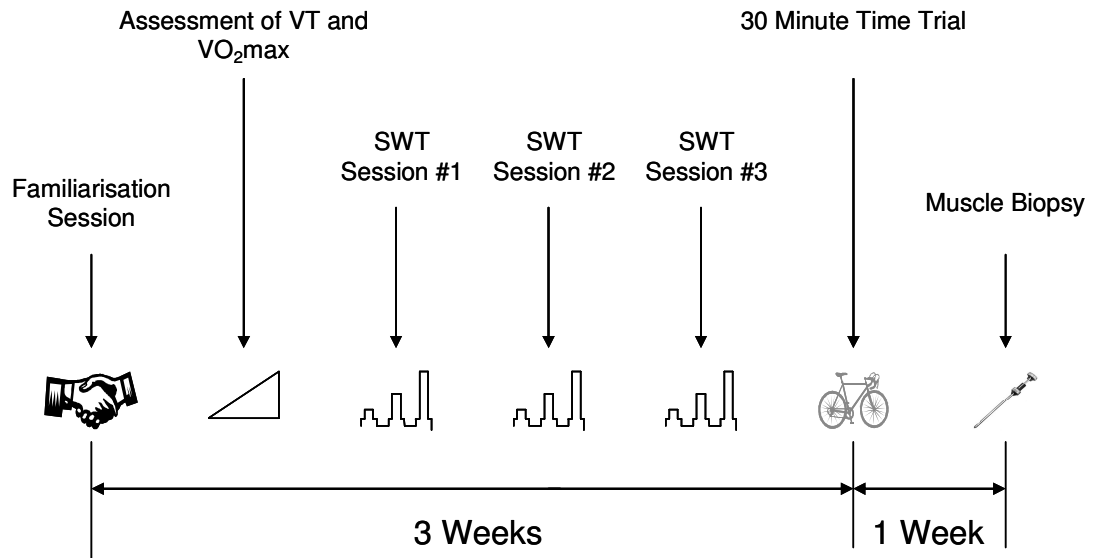


**Figure 3.1:** Schematic representation of the testing sequence throughout the series of studies.

During the first visit, informed consent, pre-exercise health screening and anthropometric assessment were completed. During this visit, the height and position of the seat and handlebars of the cycle ergometer were matched to each subject's personal bike. This position was recorded and remained consistent throughout subsequent testing sessions. The cyclists were also familiarised with all exercise procedures and equipment used in subsequent visits.

## **Assessment of Ventilatory Threshold and Maximal Aerobic Power**

At the second visit to the laboratory, each cyclist completed a ramp test to exhaustion for the determination of their VT and  $\dot{V}O_{2\max}$ . The ramp test was increased 5 W every 12 s, after an initial free wheeling period of 20 W for 3 min. The ramp test was terminated either when the cyclist could no longer maintain the required cadence or  $\dot{V}O_{2\max}$  had been attained.

VT was determined by two independent researchers using the methods of Beaver, Wasserman and Whipp (1986), where the threshold lies at the point of either:

- 1) A non-linear increase in the volume of carbon dioxide production ( $\dot{V}CO_2$ ) against  $\dot{V}E$ ; or,
- 2) An increase in expired ventilation ( $\dot{V}E$ ) with respect to  $\dot{V}O_2$  with no increase in  $\dot{V}O_2/\dot{V}CO_2$ .

$\dot{V}O_{2\max}$  was defined as the highest 30 s rolling average of the data recorded during the ramp test.  $\dot{V}O_{2\max}$  was accepted when the subjects displayed any two of the criteria of Howley, Bassett Jnr and Welch (1995) which included:

- 1) Volitional exhaustion;
- 2) Age-predicted maximal heart rate ( $220 - \text{age}$ ) ( $\pm 10 \text{ b}\cdot\text{min}^{-1}$ );
- 3) Respiratory Exchange Ratio value  $\geq 1.15$ ; or,
- 4) Plateau in oxygen consumption (increase  $< 2 \text{ mL}\cdot\text{kg}^{-1}\cdot\text{min}^{-1}$ ) with an increase in work rate.

## Square Wave Transitions

During each of the next three testing sessions, the cyclists were required to complete three sequential SWT at moderate (80% VT), heavy [50% of the difference between VT and  $\dot{V}O_{2\max}$  (50% $\Delta$ )] and severe [80% of the difference between VT and  $\dot{V}O_{2\max}$  (80% $\Delta$ )] exercise intensities (Pringle, Doust et al. 2003b). The power output for each of the three SWT intensities was calculated through the linear regression of  $\dot{V}O_2$  versus power output from the initial ramp test performed in Visit 2. The sequence of the SWT within a testing session is shown in Figure 3.2. Three repeat SWT were performed at each exercise intensity on separate days to increase the signal-to-noise ratio and ensure adequate reliability for each intensity transition (Lamarra, Whipp, Ward and Wasserman 1987; Markovitz, Sayre, Storer and Cooper 2004).

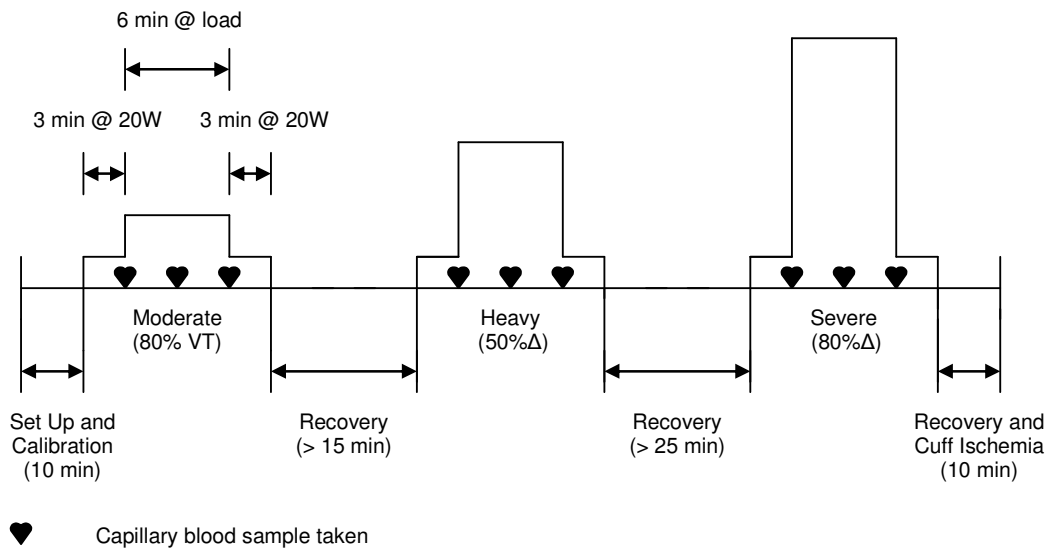


**Figure 3.2:** Schematic representation of the order of SWT within a testing session

Cyclists were given no indication of when the load was to be applied, and the load was applied instantaneously. At least 15 min rest was given

between moderate- and heavy-intensity SWT, with 25 min between heavy and severe-intensity SWT to ensure full metabolic recovery as evidence by a resting  $\dot{V}O_2$  less than  $3.5 \pm 2.0 \text{ mL}\cdot\text{kg}^{-1}\cdot\text{min}^{-1}$ .

### **30 Minute Time Trial**

During the sixth and final visit to the laboratory, all cyclists completed a 30 min time trial (30TT) to provide an index of their endurance cycling performance.

Prior to commencing the 30TT, all cyclists completed a five min warm up at 100 W and then a two min variable warm up, where the subjects self-selected their power output. Initially, all cyclists commenced the 30TT at the power output equivalent to their VT as determined during the initial ramp test (Visit 2). Throughout the 30TT, cyclists were able to freely manipulate their power output using an electric switch positioned on the handle bar of the ergometer integrated to the workload control box. Power output was manually recorded at the end of each min and the average absolute power output (W) and relative power output ( $\text{W}\cdot\text{kg BM}^{-1}$ ) were recorded as measures of cycling performance. Subjects were instructed to maintain a cadence of 90 RPM and received standardised verbal encouragement throughout the 30TT. The use of such time trial protocols has been previously shown to be reliable and display small day-to-day variation in performance of well-trained cyclists (Jeukendrup, Saris, Brouns and Kester 1996).

## PHYSIOLOGICAL MEASURES

### Expired Gas Analysis

Expired gas analysis was conducted throughout the ramp test, repeat SWT and 30TT using a *Medgraphics CPX/D* system (Medgraphics<sup>®</sup>, St Paul, MN, USA). Subjects wore a mouthpiece with saliva trap and a nose clip throughout all testing (Medgraphics<sup>®</sup>, St Paul, MN, USA). Breath-by-breath expired gas was collected using a *preVent<sup>™</sup>* pneumotach (Medgraphics<sup>®</sup>, St Paul, MN, USA) and carried through sample lines, where O<sub>2</sub> and CO<sub>2</sub> concentration was measured by high-response analysers [O<sub>2</sub>: Zirconia (<80 ms; ± 0.03% O<sub>2</sub>); CO<sub>2</sub>: infrared absorption (<130 ms; ±0.05% CO<sub>2</sub>)]. Prior to each test, the gas analysis system was calibrated with gases of known concentrations (Reference: 21 ± 0.2% O<sub>2</sub>; Calibration: 12.1 ± 0.2% O<sub>2</sub>, 5.05 ± 0.10% CO<sub>2</sub>) as per the manufacturer's instructions. The *preVent<sup>™</sup>* pneumotach has a low dead space volume (39 mL) and was calibrated before each test using a three litre syringe (Medgraphics<sup>®</sup>, St Paul, MN, USA) according to the manufacturer's instructions. Real time display of gas concentration and flow measures for each test was displayed using a personal computer. The reliability of expired gas measurements at  $\dot{V}O_{2\max}$  (TEM: 0.21 L·min<sup>-1</sup>; TEM%: 5.25%) within this laboratory was acceptable according to Gore (2000).

### Modelling of VO<sub>2</sub> Kinetics Data

#### *On-Transient Response*

The VO<sub>2</sub> data were manually examined to identify and exclude any erroneous data caused by coughing, swallowing, or breath holding. Data which were found to lie more than four standard deviations away from the mean response were deleted. The breath-by-breath data was linearly interpolated to

second-by-second values. The three repeat  $\dot{V}O_2$  responses for each of the SWT intensities (80% VT, 50% $\Delta$  and 80% $\Delta$ ) were time aligned and averaged to enhance the response characteristics which increases the signal-to-noise ratio by a factor of  $\sqrt{n}$  (Linnarsson 1974).

The non-linear least-squares regression technique was used to model the time course of the  $\dot{V}O_2$  response after the onset of exercise using either a single (Eq<sup>n</sup> 1) or double- (Eq<sup>n</sup> 2) exponential component equation as detailed below et al. 2004). Schematic representation of the modelling parameters is displayed in Figure 3.3. The initial 20 s of the  $\dot{V}O_2$  response was not included within the analysis in order to ignore the influence of the initial cardiodynamic component (Phase I) (Koppo et al. 2004).

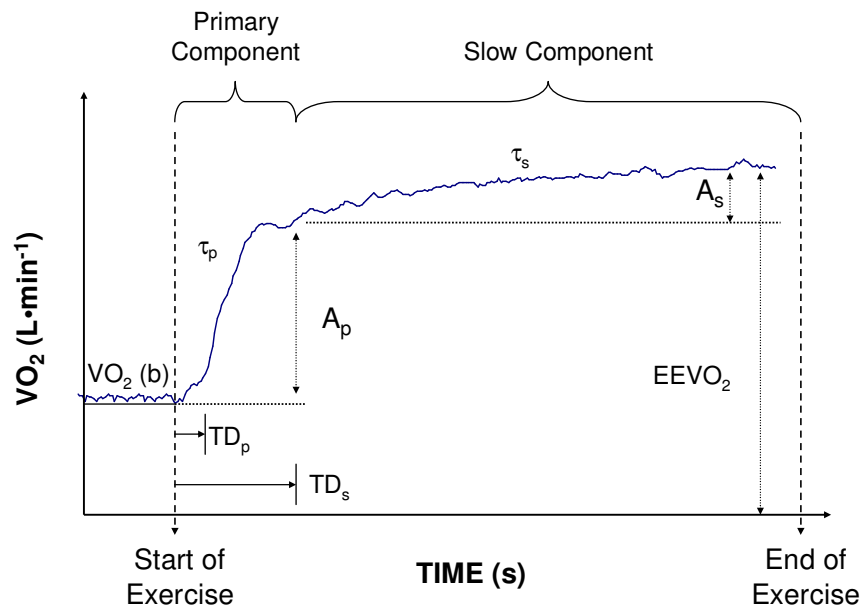


**Figure 3.3:** Schematic representation of the exponential parameters involved in modelling the on-transient  $\dot{V}O_2$  response.

*Moderate (80% VT) Intensity*

$$(Eq^n 1) \quad \dot{V}O_2 (t) = \dot{V}O_2 (b) + A_p \cdot [1 - e^{-(t-TD_p)/\tau_p}]$$

*Heavy (50%Δ) and Severe (80%Δ) Intensity*

$$(Eq^n 2) \quad \dot{V}O_2 (t) = \dot{V}O_2 (b) + A_p \cdot [1 - e^{-(t-TD_p)/\tau_p}] + A_s \cdot [1 - e^{-(t-TD_s)/\tau_s}]$$

In these equations,  $\dot{V}O_2 (t)$  is the  $\dot{V}O_2$  at a given time;  $\dot{V}O_2 (b)$  is the baseline value across the last 2 min of 'unloaded' cycling at 20 W;  $A_p$  and  $A_s$  are the asymptotic amplitudes for the primary and slow component;  $\tau_p$  and  $\tau_s$  are the time constant for each component; and  $TD_p$  and  $TD_s$  are the time delay for each component.

The use of exponential modelling to quantify the  $\dot{V}O_2$  slow component response has been reported to be a more accurate description than the outdated method of reporting the change in  $\dot{V}O_2$  between the third min of exercise and SWT completion (Bearden and Moffat 2001). The computation of best-fit parameters was performed using the 'Solver' function within Microsoft *Excel* (Microsoft Corporation™, Redmond, Washington, USA).

The overall time course of the  $\dot{V}O_2$  response to the exercise transition was determined from the weighted mean response time (wMRT) and was calculated using the methods of MacDonald, Pedersen and Hughson (1997). The wMRT was defined as the time taken to reach ~63% of the total amplitude of the response from pre-exercise  $\dot{V}O_2$  baseline to the final  $\dot{V}O_2$  plateau. The wMRT

was calculated as a weighted sum of the TD and  $\tau$  for each component, as shown below.

(Eq<sup>n</sup> 3)

$$\text{wMRT (s)} = [A_p/(A_p + A_s)] \cdot (TD_p + \tau_p) + [A_s/(A_p + A_s)] \cdot (TD_s + \tau_s)$$

In this equation, wMRT is the weighted mean response time (s);  $A_p$  and  $A_s$  are the asymptotic amplitudes for the primary and slow components component;  $\tau_p$  and  $\tau_s$  are the time constants for each component; and  $TD_p$  and  $TD_s$  are the time delays for each component.

The metabolic efficiency ( $\Delta\dot{V}O_2/\Delta W$ ) for the three SWT intensities was also examined. The  $\Delta\dot{V}O_2/\Delta W$  was calculated for the primary and slow components, as well as the total on-transient response across the three SWT intensities (Pringle et al. 2003b).

1. Primary gain ( $G_p$ ): from the start of exercise to the end of Phase II;
2. Slow gain ( $G_s$ ): from the start of the  $\dot{V}O_2$  slow component until exercise cessation;
3. Total gain ( $G_o$ ): from the start of exercise until exercise cessation.

### *Off-Transient Response*

The off-transient response was modelled for three minutes post exercise using a modified single-component exponential function as proposed by Engelen, Porszasz, Riley, Wasserman, Maehara and Barstow (1996). The off-transient modelling parameters are displayed in Figure 3.4 over the page

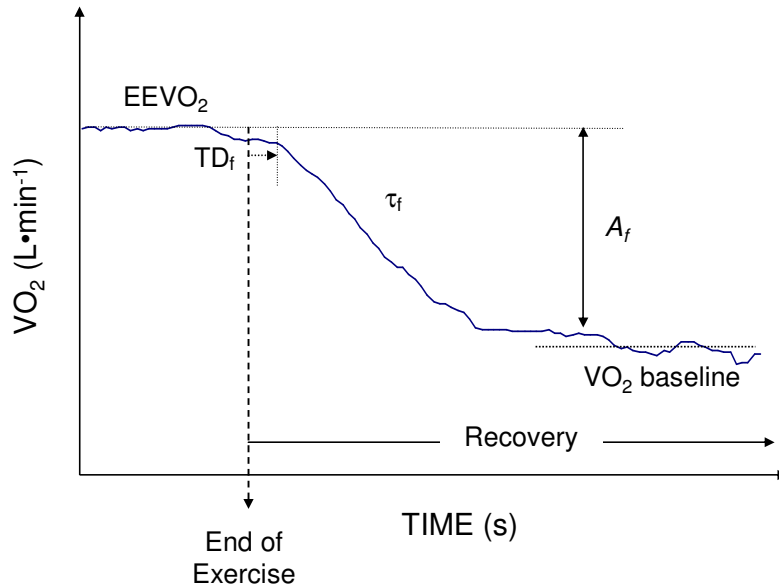


**Figure 3.4:** Schematic representation of the exponential parameters involved in modelling the off-transient  $\dot{V}O_2$  response.

$$(Eq^n 4) \quad \dot{V}O_2(t) = EE\dot{V}O_2 - A_f \cdot [1 - e^{-(t-TD_f)/\tau_f}] \cdot u_1$$

In this equation,  $\dot{V}O_2(t)$  is the  $\dot{V}O_2$  at a given time;  $EE\dot{V}O_2$  is the end-exercise  $\dot{V}O_2$  value;  $A_f$  is the asymptotic amplitude;  $\tau_f$  is the time constant and  $TD_f$  is the time delay; and  $u_1 = 0$  for  $t < TD$ ,  $u_1 = 1$  for  $t \geq TD$ .

### Near-Infrared Spectroscopy

During all testing, changes in the level of muscle oxygenation (mOxy) were monitored in the vastus lateralis (VL) using a continuous wave near infrared spectroscopy (NIRS) device (*Runman@* CWS-2000; RunMan, NIM, Philadelphia, Pa., USA) as originally described by Chance et al. (1992). A probe consisting of two light emitting diodes (760 and 850 nm) and two photodetectors is used to determine changes in the levels of oxyhemoglobin ( $HbO_2$ ) and oxymyoglobin ( $MbO_2$ ), as well as deoxygenated hemoglobin (Hb)

and myoglobin (Mb) during exercise (Figure 3.5). The distance between the light source and photodetectors remained constant at 4 cm. The scattering and absorption of the light at these wavelengths calculates the relative levels of HbO<sub>2</sub>/MbO<sub>2</sub> and Hb/Mb within the muscle tissue (Chance et al. 1992), in accordance with the modified Beer-Lambert law (Eq<sup>n</sup> 5) below.

(Eq<sup>n</sup> 5) 
$$A = \epsilon \cdot [c] \cdot l \cdot B + G$$

In Eq<sup>n</sup> 5, A is the absorption of light expressed as optical density;  $\epsilon$  is the extinction coefficient of chromophore for specific wavelength ( $\mu\text{M}/\text{cm}$ ); c = chromophore concentration ( $\mu\text{M}$ ); l = distance between point of light entry and exit (cm); B = pathlength factor of light through the tissue accounting for scattering (cm); G = geometrical correction factor to account for the geometry of tissue and optode positioning.

This calculation is dependent upon the known absorption properties of Hb, as well as the extinction coefficients of the two chromophores (Hb/Mb and HbO<sub>2</sub>/MbO<sub>2</sub>) at each wavelength. The difference between the two signals ( $\Delta 760\text{--}850\text{ nm}$ ) was used to indicate changes in mOxy.

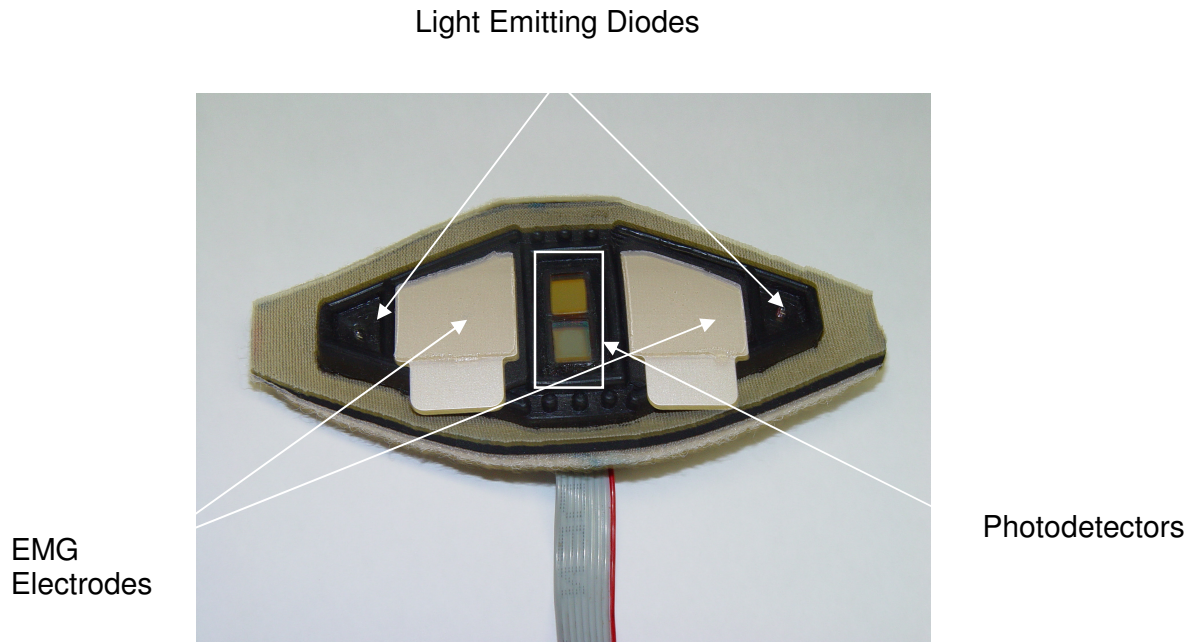


**Figure 3.5:** Modified NIRS probe for the Runman unit to allow concurrent EMG and NIRS analysis.

The modified NIRS probe was positioned 14 cm from the centre of the knee joint along the vertical axis of the thigh and over the belly of the VL in accordance with previous investigations (Chance et al. 1992; Belardinelli et al. 1995a). This position has been shown to represent a motor point within the VL and therefore reflects whole muscle activity and fibre recruitment (Kendall et al. 1993). Prior to the application of the probe, the skinfold thickness over the site was measured using *Harpender* skinfold calipers (John Bull Instruments, UK) to the nearest 0.1 mm to ensure that the signal was not affected by excessive and varying skinfold thickness (Homma et al. 1996). No significant difference was observed in the thigh skinfold thickness between the young ( $12.5 \pm 3.0$  mm) and middle-aged ( $16.2 \pm 3.6$  mm) cyclists. The probe application site was carefully shaved and a clear *Opsite*<sup>TM</sup> dressing (Smith & Nephew, London, UK) positioned over the photodetectors to prevent distortion caused by sweat

accumulation. The probe was securely bandaged to the leg using black cloth to prevent movement and to ensure that no visible light was detectable by the photodetectors. The NIRS probe was modified to incorporate the placement of two bipolar sEMG electrodes within the spacing between the light-emitting diodes and photodetectors (Figure 3.5). Pilot work within our laboratory showed that the placement of these electrodes had no effect on the NIRS signal recorded from the VL during cycling such as that used in this series of studies.

The NIRS system was interfaced with a *Labview* CB-68-LP A/D card (National Instruments, Austin, Texas, USA) and recorded at 20 Hz. Custom written *Labview* software (National Instruments, Austin, Texas, USA) was written to display and record both the 760 and 850 nm signals during testing. Prior to each exercise test, the NIRS unit was calibrated at both 760 and 850 nm wavelengths according to the manufacturer's instructions. During calibration, subjects remained in a seated position with their right leg at the bottom of the crank cycle. The  $\Delta 760\text{--}850$  nm NIRS signal was manually adjusted to a baseline value ( $0 \pm 10$  mV) so that all changes in mOxy were relative to this point. After this baseline was met, the gain was adjusted to ensure adequate signal amplification at both 760 (+500 mV) and 850 nm (-500 mV) wavelengths. The difference between these two signals was calibrated to be <10%. The NIRS signal was required to stabilise for 30 s at each calibration setting prior to acceptance.

Changes in mOxy can be semi-quantified to create normalised results compared to maximal deoxygenation and oxygenation of muscle through the application of cuff ischemia during recovery (Sahlin 1992; Miura et al. 1999;

Costes et al. 2001; Hiroyuki et al. 2002; Quaresima and Ferrari 2002a; Grassi et al. 2003). After the completion of each exercise test (i.e. ramp, SWT sequence and 30TT), a thigh cuff (Calibrated V-Lok® baunmanometer, W.A. Baum Co Inc., Copiague, New York, USA) was positioned around the superior thigh. The cuff was rapidly inflated to 250 mmHg to ensure suprasystolic pressure to overcome arterial pressure and that minimal venous blood volume was trapped in the leg musculature during arterial occlusion. The cuff pressure was maintained until the mOxy signal had reached a nadir, whereupon the cuff was quickly released to allow a hyperaemic response within the thigh. The nadir of the mOxy signal was recorded as 0% oxygenation whereas the peak mOxy observed during the hyperaemic response was recorded as 100% oxygenation. Exercise mOxy values were normalised within this scale with previous research indicating that even maximal intensity exercise values still existed within the 0-100% occlusion-hyperaemia scale (van Beekvelt et al. 2001; Quaresima and Ferrari 2002a; 2002b).

The practice of using cuff ischemia to quantify changes in mOxy has been shown previously to be both safe and reliable (Bhambhani et al. 1998). Subject's subjective pain was recorded on a ten-point Leichhardt scale throughout the cuff ischemia to monitor discomfort and pain as a safety precaution. The pain scale results of the cuff ischemia are shown in Appendix 4. The reliability of the mOxy measures at  $VO_{2max}$  was acceptable within this laboratory (TEM: 3.8 %; TEM%: 10.8%).

## Modelling of mOxy Kinetics Data

### *On-Transient Response*

The changes in mOxy were linearly interpolated to provide second-by-second values and exponential modelled to quantify the amplitude and speed of the response. The three repeat mOxy responses were time aligned and averaged to increase the signal-to-noise ratio by a factor of  $\sqrt{n}$  (Linnarsson 1974). The non-linear least-squares regression technique was used to model the time course of the on-transient mOxy responses. The on-transient mOxy responses were fitted to either a single (Eq<sup>n</sup> 6) or double exponential function (Eq<sup>n</sup> 7) for each of the three SWT intensities (80% VT, 50%Δ and 80%Δ) depending upon the observation of a slow component. The modelling parameters are schematically presented in Figure 3.6. Any data that were found to lie more than four standard deviations away from the mean response were removed. For the purposes of the present study, the curve fit was only performed if the NIRS signal fell below baseline values. The computation of best-fit parameters was performed using the Solver function within Microsoft *Excel* (Microsoft Corporation™, Redmond, Washington, USA).

$$\text{(Eq}^n \text{ 6)} \quad \text{mOxy (t)} = \text{mOxy (b)} - A_p \cdot [1 - e^{-(t-TD_p)/\tau_p}]$$

$$\text{(Eq}^n \text{ 7)} \quad \text{mOxy (t)} = \text{mOxy (b)} - A_p \cdot [1 - e^{-(t-TD_p)/\tau_p}] - A_s \cdot [1 - e^{-(t-TD_s)/\tau_s}]$$

In these equations, mOxy (t) is the mOxy at a given time; mOxy (b) is the baseline value across the last two minutes of 'unloaded' cycling at 20 W;  $A_p$  and  $A_s$  are the asymptotic amplitudes for the primary and slow components;  $\tau_p$

and  $\tau_s$  are the time constants for each component; and  $TD_p$  and  $TD_s$  are the time delays for each component.

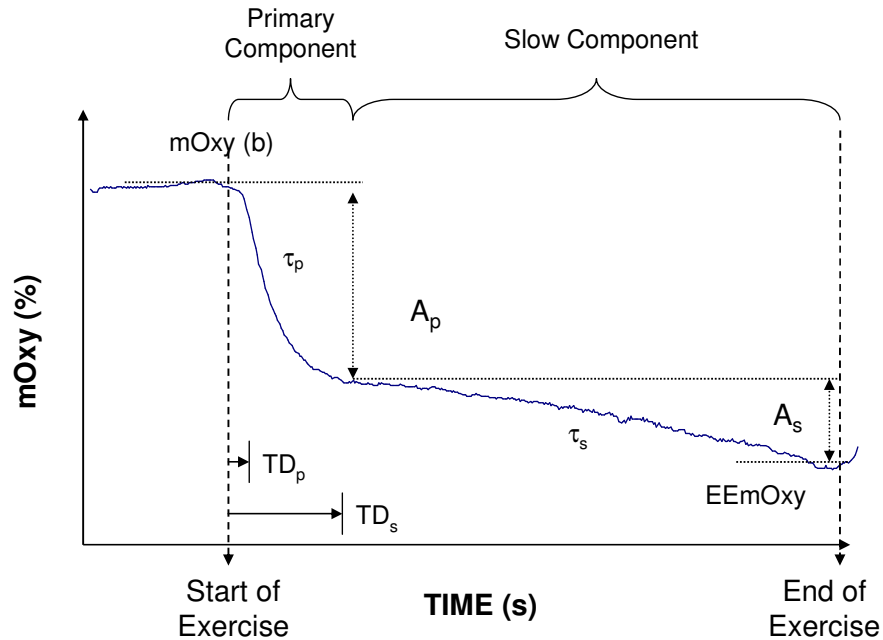


**Figure 3.6:** Schematic representation of the exponential parameters involved in modelling the on-transient mOxy response.

#### *Off-Transient Response*

The off-transient mOxy response was modelled using a single (Eq<sup>n</sup> 8) or double component (Eq<sup>n</sup> 9) exponential model with a common TD (Engelen et al. 1996). The mathematical parameters used to model the off-transient mOxy response are shown below in Figure 3.7. The function used to model the off-transient mOxy response was similar to that proposed to model the off-transient  $\dot{V}O_2$  response. The mOxy off-transient models are shown below:

$$(Eq^{\text{n}} 8) \quad mOxy(t) = EEmOxy + A_f \cdot [1 - e^{-(t-TD)/\tau_f}] \cdot u_1$$

$$(Eq^{\text{n}} 9) \quad mOxy(t) = EEmOxy + A_f \cdot [1 - e^{-(t-TD)/\tau_f}] \cdot u_1 + A_{fs} \cdot [1 - e^{-(t-TD)/\tau_{fs}}] \cdot u_1$$

In Eq<sup>n</sup> 8 and 9, the  $mOxy(t)$  is the  $mOxy$  at a given time;  $EEmOxy$  is the end-exercise  $mOxy$ ;  $A_f$  and  $A_{fs}$  are the asymptotic amplitudes of the off-transient primary and slow components;  $\tau_f$  and  $\tau_{fs}$  are the time constants;  $TD$  is the common time delay; and  $u_1 = 0$  for  $t < TD$ ,  $u_1 = 1$  for  $t \geq TD$ .

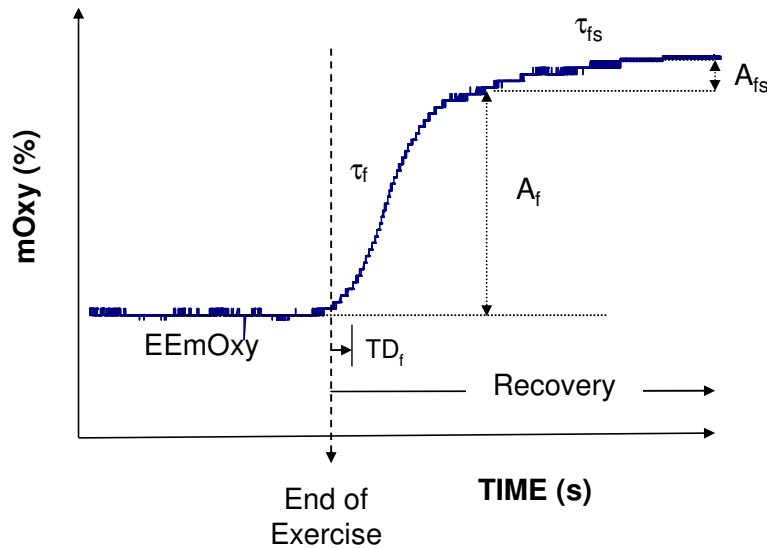


**Figure 3.7:** Schematic representation of the exponential parameters involved in modelling the off-transient  $mOxy$  response.

### Heart Rate Measurement

Heart rate was recorded telemetrically using a *Polar s610i* heart rate monitor (Polar Electro Oy, Kempele, Finland), and later downloaded to a personal computer using *Polar Advantage Software*<sup>TM</sup> version 4.0 (Polar, Electro OY, Kempele, Finland).

## **Hematological Measures**

### *Capillary Blood Sampling*

Capillary blood samples were drawn from a hyperaemic fingertip and collected into duplicate 100  $\mu$ L heparinised capillary tubes (Bacto Laboratories, Liverpool, NSW). Duplicate samples were drawn 30 s prior to SWT load application (0 min); mid-SWT (3 min) and immediately following SWT completion (6 min) of each SWT. During the 30TT, capillary samples were drawn every 10 min of cycling. Prior to sampling, the puncture site was cleansed with alcohol, dried and the first drop post-puncture was excluded from the sample. Both capillary tubes were filled simultaneously. The first sample was expelled from the capillary tube into the sample well of an *i-STAT* CG<sub>4</sub><sup>+</sup> cartridge (*i-STAT* Corporation, New Jersey, USA) and all air bubbles were removed from the sample prior to the cartridge being closed. The duplicate sample was stored on ice as a reserve until the first sample had been analysed. Both samples were discarded after one capillary tube had been successfully analysed.

### *Hematological Analysis*

All capillary blood samples were analysed for pH,  $pO_2$ ,  $[HCO_3^-]$  and  $[BLa^-]$  using *i-STAT* CG<sub>4</sub><sup>+</sup> cartridges and an *i-STAT* clinical analyser (*i-STAT* Corporation, New Jersey, NJ, USA). Prior to each testing session, the *i-STAT* analyser was self-calibrated using a routine electronic stimulation. Level 2 *i-STAT* control solution (*i-STAT* Corporation, New Jersey, NJ, USA) was also analysed following every 50 samples across testing to ensure accuracy. The *i-STAT* cartridges were stored prior to use as per manufacturer's instructions (2-8 °C), and were brought to room temperature approximately 5 min prior to

use. The *i-STAT* clinical analyser and  $CG_4^+$  cartridges have recently been shown to be reliable across the exercise intensities used in the present series of studies (Dascombe, Reaburn, Sirotic and Coutts, 2007). Results obtained using the *i-STAT*  $CG_4^+$  cartridges and analyser have shown to be reliable within our laboratory following the completion of an incremental  $\dot{V}O_{2max}$  step test [blood pH (0.02: 0.24% (TEM: TEM%));  $pO_2$  (3.15 mmHg: 3.8%);  $[HCO_3^-]$  (0.87  $mmol \cdot L^{-1}$ : 6.49%); and  $[BLa^-]$  (0.5  $mmol \cdot L^{-1}$ : 3.12%)].

### **Surface Electromyography**

Surface electromyography (sEMG) of the VL and vastus medialis (VM) was monitored to observe changes in fibre recruitment and activity across each SWT (Saunders et al. 2000; Borrani et al. 2001). sEMG data were collected from the VL and VM on the right thigh of each subject at standardised locations (Cram, Kasman and Holtz 1998). Two self adhesive Ag/AgCl electrodes (Red Dot No. 2258, 3M Medical-Surgical Division, St Paul, USA) were placed in a bipolar configuration over the belly of the VL and VM, as displayed in Figure 3.8 below. The electrodes for the VL were incorporated into the modified NIRS probe as detailed earlier in Figure 3.5 (Page 126) to ensure that the placement (14 cm superior of the patella) and inter-electrode distance of 4 cm remained consistent across testing sessions. Electrodes were aligned parallel to the direction of the muscle fibres.

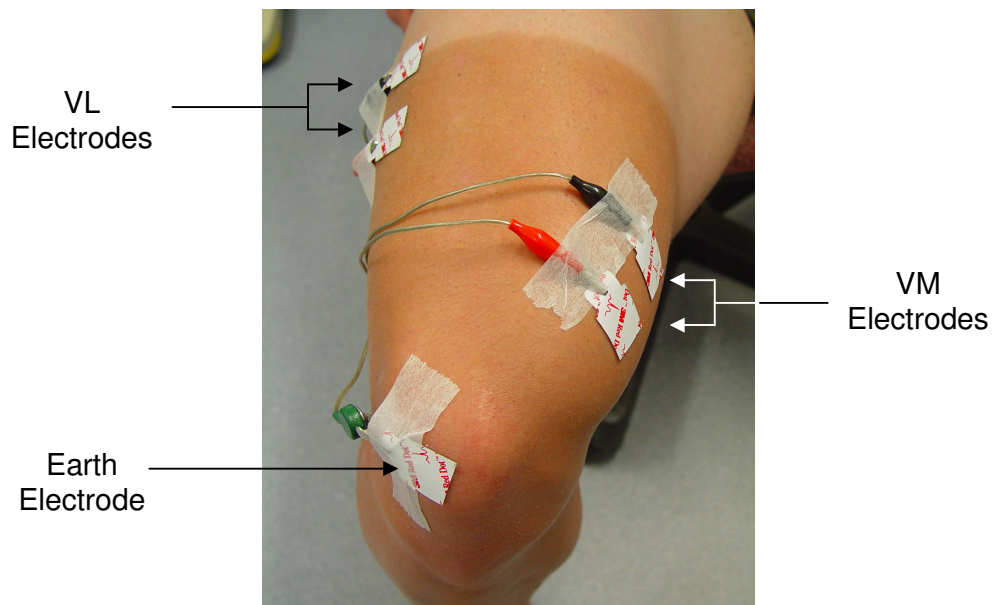


**Figure 3.8:** Illustration of the electrode placement for the VL and VM sEMG measurement.

Prior to the placement of the electrodes, the site was carefully shaved, abraded to remove the top layer of skin cells, and wiped with an alcohol swab to remove oils and salts to reduce subcutaneous impedance to less than 10 k $\Omega$ . All leads were taped down to reduce movement artefact. A single electrode was placed upon the bony surface of the patella to act as an earth contact.

The raw sEMG signal was collected during the last 10 s of each minute during both the ramp test and 30TT. During the SWT sequence testing, sEMG was recorded during the last 10 s of each 30 s across each SWT, or until volitional exhaustion during the severe-intensity SWT. The sEMG signal was recorded by an AMLAB computer system (AMLAB, Peak Performance Technologies Inc., Englewood, USA). The raw signal was amplified by a gain of 1000 and passed through an analogue to digital (A/D) card (AMLAB, Peak

Performance Technologies Inc., Englewood, USA). The signal was captured on a personal computer at 1000 Hz and processed through a 4 pole Butterworth bandpass filter with corner frequencies of 10 Hz and 450 Hz.

Crank angle was recorded simultaneously with sEMG using a custom-built coded disc attached to the crank of the Lode ergometer as shown in Figure 3.9. The coded disc had slots continually around its outer perimeter to provide an angular resolution of 5°. A slotted optical switch (Model 304-560, RS Components, Corby, UK) was used to monitor crank position in 5° increments. A separate reflective optical switch (Model 307-913, RS Components, Corby, UK) was used to recognise when the crank angle returned to 0°. The sEMG signals were only analysed for segments of the cycle stroke which had previously been shown to exhibit the greatest activity in cycling for both the VL (315-110°) and VM (305-135°) according to Jorge and Hull (1986).

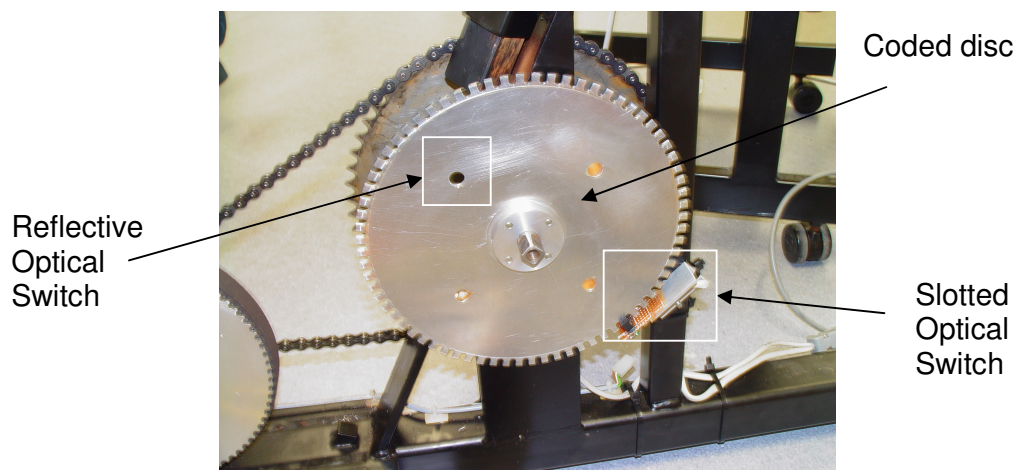


**Figure 3.9:** Configuration of the angular displacement system for the Lode Excalibur Cycle.

The sEMG activity for both VL and VM throughout this range was subsequently analysed in custom-written Labview software to determine changes in both the integrated EMG (iEMG) signal and Median Power Frequency (MPF) of each cycle stroke recorded across the 10 s collection period.

Analysis of the raw sEMG signal was performed using a Fast Fourier Transform (FFT) with a Hanning window and zero padding. iEMG was calculated by converting all amplitudes into absolute parameters, and calculating the integral for this signal across time. MPF was determined using the methods of Sparto, Parnianpour, Reinsel and Simon (1997) which utilised simple linear regression according to Eq<sup>n</sup> 10:

$$(Eq^n 10) \quad MPF = LS * time + IMF$$

In Eq<sup>n</sup> 10, MPF is the Median Power Frequency; LS is the linear slope (Hz/% total time); and, IMF is the Initial Median Frequency (Hz). An R<sup>2</sup> value of the linear regression equation was also calculated.

## **MUSCLE HISTOCHEMICAL AND ENZYMATICAL CHARACTERISTICS**

### **Muscle Biopsies**

On a separate day but within a week of completion of the last laboratory visit, two resting muscle biopsies were taken by an Orthopaedic surgeon from the mid-portion (i.e. 12-16 cm above the patella) of the right VL under local anaesthetic (0.5% *Xylocaine*) at a local medical facility. After the local anaesthetic had taken effect, the sample site was cleaned with a disinfectant

(Betadine™, Mayne Consumer Products, Baulkham Hills, NSW, Australia). A small skin incision (2-3 cm) was made through the skin and muscle fascia using a number 12 scalpel blade. A 5 mm Bergstrom biopsy needle (Stille, Sweden) was then used to obtain two muscle samples according to the method of Bergstrom (1962). To maximise muscle biopsy sample size, a length of surgical tubing connected to a 60 mL injection syringe was inserted into the proximal end of the biopsy cannula and suction applied by a co-investigator immediately prior to sampling (Evans, Pinney and Young 1982). Every effort was made to biopsy at a standardised depth of 3 cm within the muscle belly since significant differences in fibre composition have been observed between the deep and superficial fibres of the VL (Lexell et al. 1985). Immediately following the biopsy, 1-2 stitches were inserted into the incision and the thigh was wrapped with a pressure bandage. The subject was provided with post-operative instructions on wound care to minimise soreness and risk of infection. Subjects were monitored for pain and care of the biopsy site for 48 h following sampling and the results are included within Appendix 4.

The first muscle biopsy sample was removed from the biopsy cannula and orientated longitudinally under a microscope (Olympus CH-2™, Olympus Corporation, Tokyo, Japan.) in *OCT* embedding medium (TissueTek, Thuringowa, Queensland, Australia) on a cork disc and then frozen in 2-methylbutane (Sigma Number: 320404, Sigma-Aldrich Corporation, St Louis, Missouri, USA) cooled to its freezing point by liquid nitrogen (N<sub>2</sub>) for later histochemical analysis. The second biopsy sample was removed from the biopsy cannula and immediately frozen in liquid N<sub>2</sub> for later biochemical analysis. Both samples were stored in separate polypropylene cryovials (Nalge

Nunc International, Rochester, New York, USA) at -80° C until subsequent analysis.

### **Histochemistry**

Histochemical analysis of the muscle biopsies was performed at the Tissue Pathology Laboratory at the Royal Brisbane Hospital, Brisbane, Queensland, Australia. All samples were transported from Rockhampton to Brisbane in a sealed container surrounded by frozen CO<sub>2</sub> [dry ice] at -79.5° C. All histochemical staining was performed by the same qualified tissue pathologist.

### *Fibre Composition and Morphology*

Each biopsy sample was cut into serial 10 µm thick cross-sections using a Leica CM1850 cryostat (Leica Microsystems GmbH, Wetzlar, Germany) at -25° C. Fibre composition was determined by staining sections for myofibrillar adenosine triphosphatase (m-ATPase) after pre-incubation at a pH of 4.5, to allow staining of Type I, IIa and IIb muscle fibres according to the methods of Brooke and Kaiser (1970). As shown below in Figure 3.10, digital photographs (3.34 MPEG) were taken of the serial sections using a Nikon Coolpix 995 (Nikon Photo Products Inc., Tokyo, Japan) attached to a Nikon Eclipse E600 microscope (Nikon Instruments Inc., Kanagawa, Japan) at a magnification of x 20.

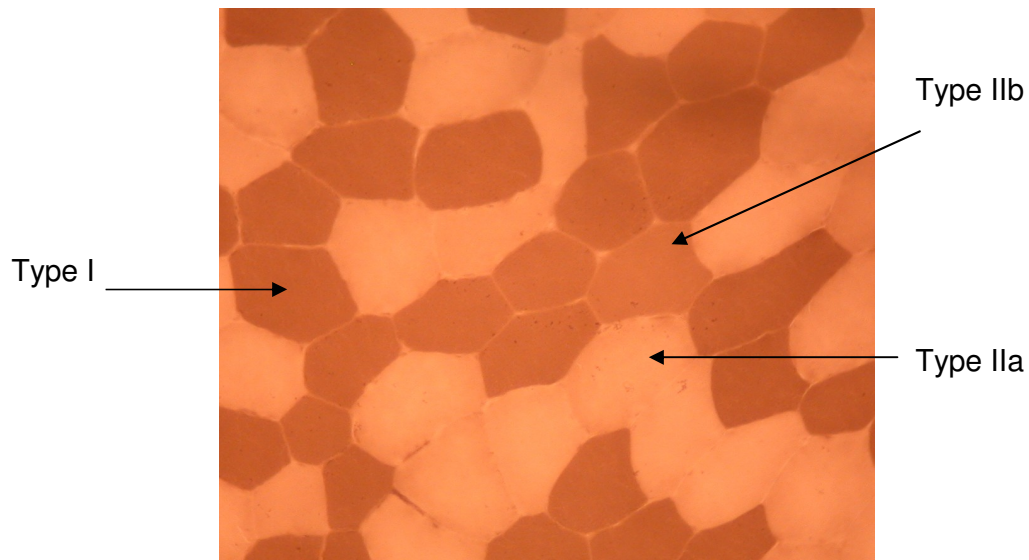


**Figure 3.10:** A typical cross-section of m-ATPase stained (pH 4.5) muscle demonstrating Type I, IIa and IIb fibres.

Percentage fibre composition was calculated using at least 200 fibres, or all countable fibres if there were fewer than 200 fibres using the public domain *Image J* program (version 1.32, U.S. National Institutes of Health, Bethesda, Maryland, USA) as counted by one operator (Blomstrand and Ekblom 1982). Two operators independently performed repeat measurements of fibre composition and demonstrated acceptable levels of intra- (TEM: 2.9%; TEM%: 5.8%) and inter-reliability (TEM: 3.9%; TEM%: 7.8%).

The cross-sectional area of at least 40 (or as many as possible if 40 were not visible) of the Type I, IIa and IIb fibres were analysed using the *Image J* software. The perimeter of the fibre was outlined and the area within the border calculated according to a constant pixel density. Prior to each fibre's measurement, the scale of measurement was calibrated using a photograph of

a 1 mm objective micrometer (Graticules Ltd, Tonbridge, Kent, UK). Only fibres without artefacts, distinct cell borders, and no tendency towards longitudinal cuts were included in the analysis (Blomstrand and Ekblom 1982). Slides were analysed in a randomized sequence and subject identity not disclosed until consensus values were obtained for all specimens. Two operators independently performed repeat measurements of morphometry and produced acceptable levels of intra- (TEM: 374.3  $\mu\text{m}^2$ ; TEM%: 4.1%) and inter-reliability (TEM: 732.7  $\mu\text{m}^2$ ; TEM%: 8.1%).

### *Capillarisation*

Additional 10  $\mu\text{m}$  cross-sections of each biopsy sample were stained using the periodic acid-Schiff (PAS) stain to visualise capillaries according to the method described by Fink and Costill (1990). Detailed photographs (3.34 MPEG) were taken of each stained section using a Nikon Coolpix 995 attached to a Nikon Eclipse E600 microscope. Capillarisation measures were performed using the *Image J* software. Analysis of capillarisation was taken directly from numerous artefact-free regions of sections until 2.0  $\text{mm}^2$  of muscle had been analysed. An example of a PAS capillarisation stain is shown below in Figure 3.11.

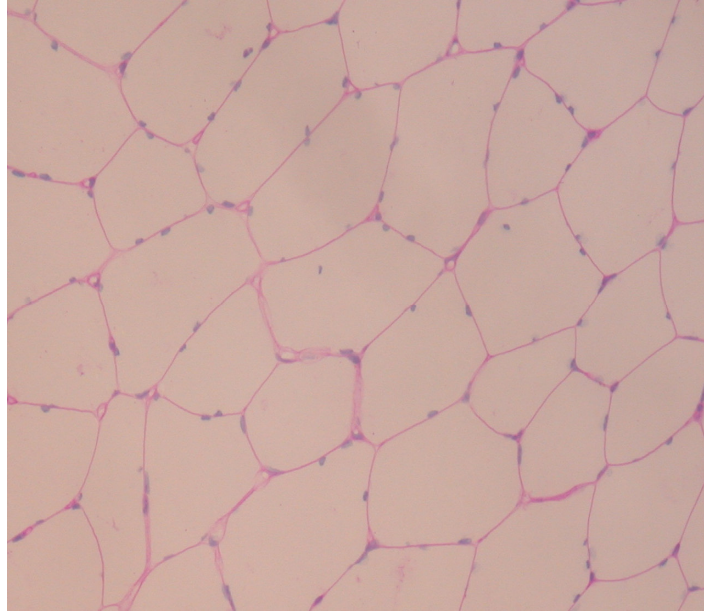


**Figure 3.11:** A typical cross-section of muscle stained for measures of capillarisation.

Capillary density ( $\text{cap}\cdot\text{mm}^{-2}$ ) was used to determine any differences in supply of capillaries to the VL within the young and middle-aged cyclists. This measure was calculated by manually counting capillaries within a randomly selected 1.0 mm square using the *Image J* software. Capillaries in contact with the borders of the grid were included within the capillary count. The capillary-to-fibre ratio (C/F) was calculated by using the grid described above and counting both the number of fibres and capillaries within the area. Capillary contacts per fibre (CC/F) was calculated by manually counting the number of capillaries in contact with individual fibres within the grid and then averaging the number per fibre. Such methods for determination of muscle capillarisation have been used in similar investigations (Chilibeck et al. 1997; Pringle et al. 2003b). Two operators independently performed repeat measurements of capillary density

and produced acceptable levels of intra- (TEM: 14.4 cap•mm<sup>-2</sup>; TEM%: 6.3%) and inter-reliability (TEM: 21.3 cap•mm<sup>-2</sup>; TEM%: 9.7%).

In order to examine the potential effects of O<sub>2</sub> diffusion capacity, both the average (DD<sub>mean</sub>) (Eq<sup>n</sup> 11) and maximum (DD<sub>max</sub>) (Eq<sup>n</sup> 12) diffusion distances were estimated using the equations developed by Snyder (1987) for capillaries distributed in random arrays.

$$(Eq^n 11) \quad DD_{mean} = \left[ \frac{0.207 + 0.232}{C:F \text{ Ratio}} \right] \times \sqrt{\text{average fibre cross-sectional area}}$$

$$(Eq^n 12) \quad DD_{max} = \left[ \frac{0.415 + 0.477}{C:F \text{ Ratio}} \right] \times \sqrt{\text{average fibre cross-sectional area}}$$

These estimates are based upon the cumulative frequency of the area of each fibre within a measured distance from a capillary. DD<sub>mean</sub> is defined as the distance to where 50% of the fibre area is served by a capillary, where DD<sub>max</sub> refers to 95% of this area. The equations employed for capillarisation were reliant upon the random distribution of capillaries throughout muscle, and based upon the C/F ratio and CC data of each fibre (Plyley and Groom 1975).

### **Enzyme Analysis**

Biochemical analysis of the muscle biopsy samples was conducted at the School of Health Sciences, Deakin University, Melbourne, Australia by the current PhD Candidate (BD). All muscle samples were transported from Rockhampton to Melbourne in a sealed container surrounded by frozen carbon dioxide (CO<sub>2</sub>) [dry ice] at -79.5° C. Upon arrival, the samples were stored at

-80° C at Deakin University. Several 5-10 mg portions of muscle were dissected and weighed on previously-calibrated Denver Instrument DI-100 electronic scales (Denver Instrument, Denver, Colorado, USA) and then stored at -80° C until homogenisation.

### *Homogenisation*

One 5-10 mg portion was removed and homogenised for the measurement of PFK and LDH activity. The sample was removed from -80° C storage and allowed to thaw on ice (0° C). A 1:50 homogenate of each muscle sample was prepared in a homogenising medium (50 mM Tris; 10mM K<sub>2</sub>HPO<sub>4</sub>; 5 mM 2-mercaptoethanol; 0.5 mM EDTA; 0.02% BSA) at pH 8.1 using a glass pestle homogeniser kept on ice. The sample was homogenised by performing 15 passes of the plunger. The homogenate was stored on ice and immediately analysed for PFK and LDH activity using the methods detailed below.

For measurement of CS and  $\beta$ -HAD activity, a separate 5-10 mg muscle sample was homogenised in a 1:50 buffer containing 0.175 M KCl and 2 mM EDTA at pH 7.4 using a *Polytron* PT 1200 homogeniser (Scientific Exchange, Manotick, Ontario, Canada). The homogenate was then freeze-thawed twice, and centrifuged at 10,000 RPM for 1 min. The supernatant of the homogenate was transferred to a 1.5 mL Eppendorf tube and stored at -80° C until subsequent analysis of CS and  $\beta$ -HAD.

A 10-15 mg sample of each muscle sample was dissected and homogenised for the measurement of 2-OGDH activity. A 1:10 homogenate was made on ice using a 50 mM Tris-HCl; 5 mM MgCl<sub>2</sub>; 1 mM EDTA

homogenising buffer at pH 8.2 using the glass pestle method described earlier. The homogenate was analysed immediately for 2-OGDH activity.

Total protein content of each homogenate was analysed using a BCA Pierce Protein Assay (Rockford, Illinois, USA). A 10  $\mu\text{L}$  aliquot of the 2-OGDH sample was diluted in 200  $\mu\text{L}$  of mixed reagent and incubated for 30 min at 37<sup>o</sup> C, and then let stand at room temperature for a further 15 min. Total protein was measured using a *Labsystems* Multiskan RC plate reader (Labsystems, Stockholm, Sweden) and *Genesis* software v4.3 (Labsystems, Stockholm, Sweden) at 550 nm. The repeatability of the BCA Pierce Protein assay was acceptable (TEM: 1.51 ( $\times 10^{-3}$ )  $\mu\text{g}\cdot\mu\text{L}^{-1}$ ; TEM%: 3.48%; CV%: 6.3%).

#### *Phosphofructokinase (PFK)*

The activity of PFK in the muscle homogenate was determined by the method of Chi et al. (1983). The homogenate was further diluted to 1:1500 in the homogenising medium containing 50 mM Tris; 10 mM  $\text{K}_2\text{HPO}_4$ ; 5 mM 2-Mercaptoethanol; 0.5 mM EDTA; 0.02% BSA at pH 8.1. A 5  $\mu\text{L}$  aliquot of the 1:1500 homogenate was added to a 0.1 mL reagent mixture (50 mM Tris, pH 8.1; 25 mM HCl; 1 mM fructose-6-phosphate; 1 mM ATP; 10 mM  $\text{K}_2\text{HPO}_4$ ; 2 mM  $\text{MgCl}_2$ ; 1 mM 2-mercaptoethanol; 0.02% BSA; 0.1 U/mL aldolase; 20  $\mu\text{M}$  NADH; 1 U/mL TPI/ $\alpha$ -GPDH) in separate borosilicate glass culture tubes (Kimble, Vineland, New Jersey, USA). Each tube was immediately mixed by vortexing (Ratek VM1 Vortex<sup>TM</sup>, Ratek Instruments Pty. LTd., Boronia, Victoria, Australia) and then incubated at room temperature for 1 h. Next, 10  $\mu\text{L}$  of 0.75M HCL was added to each tube, briefly mixed by vortexing and incubated for a further 10 min at room temperature. After this incubation, 1 mL of a 6 M

NaOH-10 mM Imidazole solution was added to each tube, and mixed thoroughly by vortexing. The tubes were then placed in a *Grant Y6* water bath (Grant Instruments Cambridge Ltd., Herts, UK) set at 60° C for 20 min. Following this, the tubes were transferred to a water bath at room temperature for a further 10 min. Each tube was then dried. The absorbance of NADH was read (at 340 nm excitation and 465 nm emission) on an *Optical Technology Devices Inc. Ratio 2* filter fluorometer (Optical Technology Devices, Valhalla, NY, USA).

PFK activity was determined through NADH reduction to NAD, and was calculated through the equation below (Eq<sup>n</sup> 13). Blanks and working fructose-1,6-biphosphate standard solutions of 1 μM, 2.5 μM and 3.5 μM were also measured to provide a standard curve and allow quantification of the assay. All samples were measured in triplicate and the mean taken for data analysis. The absolute (μmol•g<sup>-1</sup>•min<sup>-1</sup>) and specific (μmol•g<sub>protein</sub><sup>-1</sup>•min<sup>-1</sup>) activity of PFK was calculated for each muscle sample. The repeatability of the PFK assay was acceptable (TEM: 0.86 μmol•g<sup>-1</sup>•min<sup>-1</sup>; TEM%: 2.46%; CV%: 2.6%).

(Eq<sup>n</sup> 13)

$$\text{PFK Activity } (\mu\text{mol/g/min}) = \left( \frac{F_{\text{sample}}}{F_{\text{standard}}} \right) \times (\text{mM}_{\text{standard}} \times \text{mL}_{\text{standard}}) \div \text{g}_{\text{wet muscle}} \div \text{min}$$

Where:  $F_{\text{sample}}$  = fluorescence of sample;  $F_{\text{standard}}$  = fluorescence of standard;  $\text{mM}_{\text{std}}$  = concentration of standard;  $\text{mL}_{\text{standard}}$  = volume of standard;  $\text{g}_{\text{wet muscle}}$  = wet mass of tissue within sample; min = time of incubation prior to addition of HCl.

### *Lactate Dehydrogenase (LDH)*

LDH activity was measured using the method of Chi et al. (1983). Immediately after homogenisation, the sample was centrifuged at 3000 g for 15 min at 4°C. A 40 µL aliquot of homogenate supernatant was added to 1 mL of a 200 mM imidazole-0.1% BSA buffer at pH 7.0 (1:1250). A 100 µL volume of reagent mixture (0.1 M imidazole; 1 M HCl; 2 mM pyruvate; 0.05% BSA; 0.3 mM NADH at pH 7.0) was added to triplicate Kimble tubes (Kimble, Vineland, New Jersey, USA). The reaction was started by adding 1 µL of the muscle homogenate supernatant to each Kimble tube, and immediately mixed by vortexing. The samples were then incubated at room temperature for 1 h. 10 µL of 1 M HCl was then added to the mixture and the assay was let stand at room temperature for a further 10 min. After this, 1 mL of 6 M NaOH-10mM imidazole mixture was then added to each Kimble tube and immediately mixed by vortexing. Samples were then placed in the *Grant Y6* water bath set at 60° C for 20 min. Following this, the tubes were transferred to a water bath at room temperature for a further 10 min. Each tube was then dried. The absorbance of NADH was read (at 340 nm excitation and 465 nm emission) on an *Optical Technology Devices Inc. Ratio 2* filter fluorometer.

LDH activity was measured through the change in fluorescence as a result of NADH reduction to NAD, using the formula below (Eq<sup>n</sup> 14). Blanks and working NAD standards of 25 µM, 50 µM and 75 µM were measured to provide a standard curve and allow quantification of the assay. All samples were measured in triplicate and the mean taken for data analysis. The absolute ( $\mu\text{mol}\cdot\text{g}^{-1}\cdot\text{min}^{-1}$ ) and specific ( $\mu\text{mol}\cdot\text{g}_{\text{protein}}^{-1}\cdot\text{min}^{-1}$ ) activity of LDH was calculated

for each muscle sample. The repeatability of the LDH assay was acceptable (TEM: 4.14  $\mu\text{mol}\cdot\text{g}^{-1}\cdot\text{min}^{-1}$ ; TEM%: 2.74%; CV%: 3.0%).

(Eq<sup>n</sup> 14)

$$\text{LDH Activity } (\mu\text{mol/g/min}) = \left( \frac{F_{\text{sample}}}{F_{\text{standard}}} \right) \times (\text{mM}_{\text{standard}} \times \text{mL}_{\text{standard}}) \div \text{g}_{\text{wet muscle}} \div \text{min}$$

Where:  $F_{\text{sample}}$  = fluorescence of sample;  $F_{\text{standard}}$  = fluorescence of standard;  $\text{mM}_{\text{std}}$  = concentration of standard;  $\text{mL}_{\text{standard}}$  = volume of standard;  $\text{g}_{\text{wet muscle}}$  = wet mass of tissue within sample; min = time of incubation prior to addition of HCl.

#### *Citrate Synthase (CS)*

The activity of CS was measured using the method reported by Chi et al. (1983). The reagent mixture consisted of 100 mM Tris (pH 8.3), 50  $\mu\text{L}$  of 1 mM DTNB, and 80  $\mu\text{L}$  of 3 mM acetyl-CoA. A 330  $\mu\text{L}$  volume of reagent mixture and 10  $\mu\text{L}$  of muscle homogenate were added together in 10 mL quartz cuvettes (Starna Pty Ltd, Baulkham Hills, NSW, Australia). The cuvettes were then inserted in a *Helios Unicam* spectrophotometer (Unicam Spectrometry, Cambridge, UK) set to 412 nm set at a temperature of 25<sup>o</sup> C. All cuvettes were allowed to pre-incubate at 25<sup>o</sup>C for 5 min. To commence the reaction, 30  $\mu\text{L}$  of 10mM oxalacetate was added into each cuvette, and mixed by gentle inversion. Each cuvette was then placed back into the spectrophotometer, zeroed and then the change in DTNB absorbance was recorded at 15 s intervals for 3 min. For the measurement of the blank sample, the identical procedure was performed as for the reagent mixture and muscle homogenate, but no

oxalacetate was added. The activity of CS was then calculated using the equation below (Eq<sup>n</sup> 15), based upon the changes within absorbance of DTNB as measured by the spectrophotometer. All samples were measured in duplicate and the mean value used for data analysis. The absolute ( $\mu\text{mol}\cdot\text{g}^{-1}\cdot\text{min}^{-1}$ ) and specific ( $\mu\text{mol}\cdot\text{g}_{\text{protein}}^{-1}\cdot\text{min}^{-1}$ ) activity of CS was calculated for each muscle sample. The reliability of the CS assay was acceptable (TEM:  $1.69 \mu\text{mol}\cdot\text{g}^{-1}\cdot\text{min}^{-1}$ ; TEM%: 8.39%; CV%: 8.4%).

(Eq<sup>n</sup> 15)

$$\text{CS Activity } (\mu\text{mol/g/min}) = \frac{\Delta\text{Abs/min} \times \text{Total volume}}{\text{Sample volume} \times 13.6} \times \text{Dilution factor}$$

Where:  $\Delta\text{Abs/min}$  = average change in absorbance per minute; Total volume = total volume of cuvette; Sample volume = volume of sample in cuvette; Dilution factor = magnitude of sample dilution;  $13.6 \text{ M}^{-1}\cdot\text{cm}^{-1}$  = the molar extinction coefficient of DTNB at 412 nm.

#### *$\beta$ -Hydroxyacyl-CoA Dehydrogenase ( $\beta$ -HAD)*

$\beta$ -HAD activity was determined using the method of Chi et al. (1983). A 430  $\mu\text{L}$  volume of reagent mixture (1 M Tris-HCl (pH 7.0); 200 mM EDTA; 5 mM NADH) and 10  $\mu\text{L}$  of a 10% Triton X-100 solution (0.5 mL Triton x 100; 2 mL Ethanol; 2.5 mL  $\text{H}_2\text{O}$ ) were added to 10 mL quartz cuvettes (Starna Pty Ltd, Baulkham Hills, NSW, Australia). Next a 50  $\mu\text{L}$  volume of muscle homogenate was also added to the cuvette, which was then placed and pre-incubated at 30° C for 5 min. The decrease in NADH absorbance was measured by a *Helios Unicam* spectrophotometer set at 340 nm at 30°C. Prior to the reaction being

triggered, the changes in NADH production were recorded for 2 min to enable each cuvette to act as its own control. To start the reaction, 10  $\mu\text{L}$  of acetoacetyl-CoA was added to each cuvette and mixed through gentle inversion. The reduction in NADH was recorded in 15 s intervals across 4 min.  $\beta$ -HAD activity was calculated using the equation below (Eq<sup>n</sup> 16). All samples were measured in triplicate and the mean taken for analysis. The absolute ( $\mu\text{mol}\cdot\text{g}^{-1}\cdot\text{min}^{-1}$ ) and specific ( $\mu\text{mol}\cdot\text{g}_{\text{protein}}^{-1}\cdot\text{min}^{-1}$ ) activity of  $\beta$ -HAD was calculated for each muscle sample. The reliability of the  $\beta$ -HAD assay was found to be acceptable (TEM:  $0.58 \mu\text{mol}\cdot\text{g}^{-1}\cdot\text{min}^{-1}$ ; TEM%: 9.35%; CV%: 8.5%).

(Eq<sup>n</sup> 16)

$$\beta\text{-HAD Activity } (\mu\text{mol/g/min}) = \frac{\Delta\text{Abs/min} \times \text{Total volume}}{\text{Sample volume} \times 6.22} \times \text{Dilution factor}$$

Where:  $\Delta\text{Abs/min}$  = average change in absorbance per minute; Total volume = total volume of cuvette; Sample volume = volume of sample in cuvette; Dilution factor = magnitude of sample dilution;  $6.22 \text{ M}^{-1}\cdot\text{cm}^{-1}$  = the molar extinction coefficient of NADH at 340 nm.

#### *2-Oxoglutarate Dehydrogenase (2-OGDH)*

The activity of 2-OGDH within the muscle samples was measured using the method of Blomstrand, Radegran and Saltin (1997). Firstly, 675  $\mu\text{L}$  of a reaction mixture containing 50 mM triethanolamine; 0.05% Triton; 10  $\mu\text{M}$  Rotenone at pH 7.4 and further volumes of 50  $\mu\text{L}$  of 40 mM NAD, 50  $\mu\text{L}$  of 40 mM 2-oxoglutarate and 25  $\mu\text{L}$  of 16 mM CoA were added to a 10 mL quartz cuvette. The cuvette was allowed to pre-incubate for 5 min in the

spectrophotometer at 25° C. Next, 25 µL of muscle homogenate was added to the cuvette to start the reaction. 2-OGDH activity was measured through the production of NADH measured using a *Helios Unicam* spectrophotometer set at 340 nm at 25° C. Changes in NADH production were monitored in 15 s intervals across 3 min. 2-OGDH activity was calculated using the equation detailed below (Eq<sup>n</sup> 17). Prior to the addition of muscle homogenate, the changes in NADH production were recorded for 2 min to enable each cuvette to act as its own control. All samples were measured in triplicate and the mean value taken for later data analysis. The absolute ( $\mu\text{mol}\cdot\text{g}^{-1}\cdot\text{min}^{-1}$ ) and specific ( $\mu\text{mol}\cdot\text{g}_{\text{protein}}^{-1}\cdot\text{min}^{-1}$ ) activity of 2-OGDH was calculated for each muscle sample. The reliability of the 2-OGDH assay was acceptable (TEM: 0.11  $\mu\text{mol}\cdot\text{g}^{-1}\cdot\text{min}^{-1}$ ; TEM%: 7.62% CV%: 9.1%).

(Eq<sup>n</sup> 17)

$$\text{2-OGDH Activity } (\mu\text{mol/g/min}) = \frac{\Delta\text{Abs/min} \times \text{Total volume}}{\text{Sample volume} \times 6.22} \times \text{Dilution factor}$$

Where:  $\Delta\text{Abs/min}$  = average change in absorbance per minute; Total volume = total volume of cuvette; Sample volume = volume of sample in cuvette; Dilution factor = magnitude of sample dilution;  $6.22 \text{ M}^{-1}\cdot\text{cm}^{-1}$  = the molar extinction coefficient of NADH at 340 nm.

## STATISTICAL ANALYSIS

Means and standard deviations ( $\bar{X} \pm \text{SD}$ ) were determined for all parameters of interest. In order to determine the likelihood of a Type I error, a Greenhouse-Geisser adjustment was performed to ensure the sphericity of all

measures. The continuous variables were assessed using a Kolmogorov-Smirnov test of homogeneity to ensure all data were normally distributed.

Independent sample *t*-tests were used to detect any between-group differences (e.g. young and middle-aged cyclists) in the anthropometric, physiological, histochemical and biochemical characteristics. Data variance was assessed using a Levene's Test. The observed differences were supported using Cohen's D effect size comparisons and 95% confidence intervals (CI) were calculated for all data. The magnitude of the observed differences was quantified using effect size statistics ( $\eta^2$ ) as described by Cohen (1992), where the values of 0.6, 0.8, 1.0 and >1.0 were representative of small, medium, large and very large effect sizes, respectively.

Significant differences in  $\dot{V}O_2$  and mOxy kinetic parameters between groups (young and middle-aged) and across intensities (moderate, heavy and severe) were identified using 2 x 3 Repeated Measures Analysis of Variance (RMANOVA). A 2 x 2 RMANOVA was used to determine differences in the kinetic parameters between groups (age) and physiological measures ( $\dot{V}O_2$  and mOxy) for each SWT intensity. 2 x 2 RMANOVA were also used to detect significant changes within kinetic parameters across the on- and off-transient responses at each SWT intensity. Significant changes within the hematological parameters and blood gases were also examined using 2 x 3 RMANOVA to report upon the effect of both age and time. Similarly, 2 x 3 RMANOVA's were used to examine the effect of age and time within a number of physiological variables measured across the 30TT.

For all multivariate tests, the mean F statistic was used to identify the level of significance between group effects of age, and within-group effects of intensity adjusted by the Greenhouse-Geisser epsilon values in the event of violation of the sphericity assumption. Following each RMANOVA, a Least Significant Differences (LSD) *post-hoc* comparison was utilised to detect the location of any significant differences observed across intensities. The magnitude of the observed differences across groups and intensities was quantified using effect size statistics ( $\eta^2$ ) as described by Cohen (1992), where the values of 0.6, 0.8, 1.0 and >1.0 were representative of small, medium, large and very large effect sizes, respectively.

Multiple Pearson product-moment correlations ( $r$ ) were used to investigate the relationships between anthropometric, physiological, histochemical and enzymatic parameters,  $\text{VO}_2$  and mOxy kinetic parameters, hematological parameters and 30TT performance measures within each age group.

The measures of reliability [Technical Error of Measurement (TEM); Technical Error of Measurement Percentage (TEM%) and Co-efficient of Variation (CV%)] used to assess the methods outlined in this chapter were calculated in accordance with the method of Norton and Olds (1996). Methodological procedures were deemed reliable if both the TEM% and CV% were less than 10%. All statistical calculations were performed using Statistical Package for Social Statistical software (version 11, SPSS Inc., Chicago, Illinois, USA). Statistical significance was accepted using an alpha ( $p$ ) level of 0.05.